Fuel Cells
FROM FUNDAMENTALS TO SYSTEMS

ORIGINAL RESEARCH PAPER

Ni migration in solid oxide cell electrodes: Review and revised hypothesis

Mogens B. Mogensen PhD[1] | **Ming Chen PhD[1]** | **Henrik Lund Frandsen PhD[1]** |
Christopher Graves PhD[1,2] | **Anne Hauch PhD[1]** | **Peter Vang Hendriksen PhD[1]** |
Torben Jacobsen PhD[3] | **Søren Højgaard Jensen PhD[4,5]** | **Theis Løye Skafte PhD[1,6]** |
Xiufu Sun PhD[1]

[1] Department of Energy Conversion and Storage, Technical University of Denmark (DTU), Lyngby, Denmark

[2] Noon Energy Inc., Palo Alto, California, USA

[3] Department of Chemistry, Technical University of Denmark (DTU), Lyngby, Denmark

[4] DynElectro Aps, Gadstrup, Denmark

[5] Department of Energy Technology, Aalborg University, Aalborg, Denmark

[6] Energy Conversion Group, Lawrence Berkeley National Laboratory, Berkeley, California, USA

Correspondence
Mogens B. Mogensen, Department of Energy Conversion and Storage, Technical University of Denmark (DTU), Fysikvej, Building 310, DK-2800 Kgs. Lyngby, Denmark.
Email: momo@DTU.dk

Abstract

Severe degradation of Ni-YSZ (yttria stabilized zirconia) electrodes of solid oxide cells (SOCs) due to Ni migration is well known, but the literature contains apparent contradictions. The mechanisms are still under debate. Fine structured Ni-YSZ composite electrodes often degrade at operation temperature (700–950°C), because Ni particles lose electrical contact with each other as larger Ni-particles grow on the expense of smaller ones. Another type of Ni migration, which may be very damaging, is the relocation of Ni in the most active part of the Ni-YSZ cermet electrode next to the dense YSZ electrolyte. Emphasis is put on the migration of Ni away from the YSZ electrolyte in solid oxide electrolysis cells (SOECs). This is seen as an important obstacle to the commercialization of SOC systems.

Apart from temperature, degradation of Ni-YSZ electrodes in SOCs is related to Ni-YSZ electrode overpotential and the local redox potential of the gas mixture inside the porous Ni-YSZ electrode. A unifying Ni migration mechanism is proposed, and methods of alleviating the electrode degradation are discussed. The hypothesis is that Ni migrates via surface diffusion of $Ni(OH)_x$ species below ca. 800°C and via $Ni(OH)_x$ species in gas phase above ca. 900°C.

KEYWORDS

effect of impurities, effect of overpotential, effect of oxygen potential, nickel (Ni) migration, SOEC degradation, solid oxide cell (SOC), solid oxide electrolysis cell (SOEC), solid oxide fuel cell (SOFC)

1 | INTRODUCTION

The solid oxide cell (SOC) is reversible, that is, it operates very well as both solid oxide fuel cell (SOFC) and as solid oxide electrolyzer cell (SOEC). The reversible SOC is often abbreviated reversible solid oxide cell. It has a great potential as converter for renewable electricity to fuels or chemicals (Power-to-X), but better durability of SOECs is still needed in order to widely commercialize SOCs. Ni has two

main functions in high performing types of SOCs such as bipolar flat plate SOCs: (i) It serves as an electrocatalyst in the fine structured Ni-YSZ (yttria stabilized zirconia) cermet fuel electrode, and (ii) it provides an electron conducting current collector function through the coarse structured Ni-YSZ cermet support. Ni works well for both functions. It is necessary that optimal structures are obtained in the manufacturing and maintained during the lifetime of the cell in order to get and keep high cell performance.

However, Ni has a high mobility in the operation temperature range of 650–950°C, which is typical for SOCs, and it seems still difficult to control the optimal Ni structure over many years at high cell polarization/high current density.

Several kinds of Ni migration in Ni-YSZ electrodes of SOCs have been reported in the literature. The characteristics of the various Ni migration types are apparently of different nature. An early careful study of high migration rate of Ni was in particle coarsening in Ni-YSZ cermet electrodes [1]. Another one is Ni migration out of Ni-YSZ composite cermet electrodes in SOFCs [2], and a third is that Ni in the active Ni-YSZ fuel electrode layer of SOECs adjacent to the YSZ electrolyte is migrating away from the electrolyte toward the Ni-YSZ support leaving an inactive Ni depleted zone [3]. Furthermore, apparent contradicting experimental evidences have been reported as described below.

Growth of microscopic Ni particles supported in porous ceramics in gaseous atmospheres will, like for most metals, follow one or both of two basic mechanisms: (i) Ostwald ripening, which is single atom or molecule migration, where Ni atoms are emitted from one Ni particle, migrate over the support or in the vapor phase, and get captured by another particle, (ii) Ni particle migration over the support followed by coalescence with other Ni clusters (PMC). In case of no other driving forces then for both cases the transport of Ni will be driven by Ni surface energy difference between small and large particles. It will make the larger Ni particles grow larger, and the small ones get smaller and finally disappear leading to an overall coarsening of the microstructure. In case of presence of significant gradients, for example, in partial pressure gradients in reactive gases or electrochemical gradients, the migration of metal may be more complex, even though it will usually end up with coarse metal particles in some areas and no or little metal in other. Ni particle coarsening seems in all cases to contribute to degradation of Ni-cermet electrodes in SOC as Ni particle coarsening correlates well with degradation of the electrical conductivity of cermets [1,4]. The electronic conductivity is normally not limiting the cell performance, but in general a certain loss of active three phase boundary (3PB), that is, decrease in electrochemically active sites per electrode volume, is also associated with Ni particle coarsening, and this may affect the area specific polarization resistance of the electrode.

This paper gives a review of selected experimental and model reports on migration of Ni inside porous YSZ, in gadolinia doped ceria (CGO) in SOCs, and one example of Ni in a $MgAl_2O_4$ catalysts. It is neither possible nor suitable to cover all available literature on this subject. Nevertheless, we have endeavored to cover most important aspects of this issue in order to understand the mechanism and to explain the apparently contradictory experimental reports and differences in conceptions of mechanisms. Some emphasis is put on the degradation related to SOEC as many researchers think that this degradation of the Ni-based fuel electrode is the most important issue to be solved in order to boost SOEC commercialization.

2 | SELECTED LITERATURE DATA

Unless otherwise stated, all data described in this review are from flat-plate-Ni-YSZ fuel electrode supported cells or from electrolyte supported cells, which are the main types of SOC during the recent couple of decades. These two types have similar thin and fine structured active fuel electrodes and are therefore reasonably comparable.

2.1 | Coarsening of non- or low-polarized Ni particles in cermets

Simwonis et al [1] studied a relatively coarse type of Ni-cermet prepared from 56 wt.% NiO and 44 wt.% 8YSZ giving 40 vol.% Ni and 60 vol.% YSZ after reduction of NiO to Ni. They found an increase of average Ni particle size from about 2 μm to 2.6 μm after 4000 h in Ar/4% H_2/3% H_2O at 1000°C. This relatively small increase in Ni particle size caused a decrease in electrical conductivity of the Ni-YSZ cermet (measured at room temperature) of 33.3% indicating a significant loss of Ni-Ni particle contacts during the particle growth. In turn, such large decrease in loss of Ni-Ni-particle contacts as a consequence of a small increase in particle size indicates that agglomeration of Ni particles occurred. An agglomeration involves migration of Ni. In other words, connection between a significant fraction of Ni-particles is lost due to the Ni migration. It is also important to note that 40 vol.% Ni is not far from the electron percolation threshold of about 30 vol.% [5]. Furthermore, the total length of active 3PB between gas phase, Ni, and YSZ electrolyte that facilitate the electrochemical reaction, will decrease with decreasing number of particles and increasing particle size for a given amount of Ni.

Pihlatie et al [4] studied the Ni particle growth in two atmospheres: (i) p(Ar) = 0.70, p(H_2) = 0.15, p(H_2O) = 0.15 bar, and (ii) Ar exchanged with He, but with same H_2 and H_2O partial pressures as in (i). The temperature was 850°C, and the electrical conductivity of the cermets decreased by more than 50% within less than 50 h. It was found that the particle growth was dependent on type of inert gas applied, that is, the Ni-particles grew faster in the gas with He than in the one with Ar. A change of a majority of inert gas from a heavy atomic weight to a low one will increase the diffusion rate of minority species in the gas. Thus, this result indicates that at least part of the observed

Ni migration behind Ni particle growth and Ni-Ni contact loss originates from gas phase Ni transport. Furthermore, it was also found by low voltage scanning electron microscopy (LV-SEM) that many Ni-Ni-particle contacts were lost during test. A description of LV-SEM, which in particular is a very strong tool for posttest examination of metal cermet electrodes, can be found in the work by Thydén et al. [6]. Holzer et al [7] found that Ni particle growth in Ni-CGO cermets at 1050°C was much faster (140% per initial 100 h) in humid atmosphere (60 vol.% H_2O, 40 vol.% [85.5 N_2/14.5 H_2]) than in dry gas (97 vol.% N_2, 3 vol.% H_2), where it was about 1% per initial 100 h. The particle growth practically stopped after 1000 h in the humid gas indicating the simple Ostwald ripening mechanism, that is, growth through direct Ni-Ni particle contact and driven by minimization of the free surface energy gain associated with the smaller surface area per mol of large particles. However, also gas flow rate had a strong effect on the degradation rate, which more points to an Ostwald ripening mechanism of evaporation-condensation of gaseous species. The particle growth kinetics will expectedly develop over time similarly for the two cases.

The above results [1,4,7] have later been confirmed by a number of studies using two dimension (2D) SEM micrographs from pristine and tested Ni-YSZ cermet fuel electrodes in SOCs. It seems to be generally agreed that Ni particle growth takes place during SOC operation and that the length of connected electrochemically active 3PB decreases both in SOFC and SOEC mode, when the cell is operated for extended times [8–16]. As it will be clear from the following section, this is only the case in regions of the Ni-YSZ electrode without Ni migration over "long distance" of more than 1 μm (the size of 1–2 Ni particles), which is only observed very near the dense YSZ electrolyte. In other words, Ni particle coarsening is not affected by current direction or current density if no essential local electrochemistry occurs.

During the recent decade several researchers in Ni-YSZ cermet electrodes have been using 3D methods such as X-ray nano computed tomography (nano-CT) plus differential absorption imaging [14,16] and focused ion beam combined with SEM (FIB-SEM) plus energy dispersive X-ray spectroscopy (EDS) [9,17]. Hubert et al [18] performed Ni particle growth tested over periods of 1000–9000 h at temperatures of 750 and 850°C. A gas inlet composition of 50% H_2 + 50% H_2O was supplied to the fuel electrode, and the cells were long-term tested with constant current density of plus (SOFC) or minus (SOEC) 0.5 A cm^{-2}. After the aging test, characterization of the Ni-YSZ cermet electrodes using nano-CT and SEM revealed that Ni particle coarsening during 2000 h at 850°C induced a significant decrease in density of Ni-YSZ-fuel gas three phase

boundary length (3PBL). The Ni to gas-specific surface area decreased to 40% of the starting value, whereas the contact surface area between Ni and YSZ was not changed. The latter implies that Ni sintering is restricted by the YSZ backbone, which is extremely stable.

The 3D investigations have quantified the Ni particle growth and loss of 3PBL. However, not all 3D results are agreeing very well. This may for example be due to: i) sample volumes investigated are not representative for the structure under examination, ii) Ni-YSZ cermet sintering behavior may differ because of small differences in composition, structure, and content of impurities. However, all 3D results look still also somewhat uncertain, and the literature data are not agreeing very well. Yet, it confirms the more qualitative findings from the 2D investigation, for example, strong particle growth may decrease the 3PBL with a factor of about 2 [17]. Furthermore, it is clear that the Ni grain growth is very much restricted by the porous YSZ, and the detailed Ni-YSZ sintering history and resulting structure have a strong effect on Ni particle growth as for example, shown by Chen-Wiegart et al. [19]. They studied in situ Ni-particle growth in Ni-YSZ cermets in humidified hydrogen at 1050°C after 0, 12, 24, 48, and 92 h using nano-CT with sub-100 nm resolution and found: (i) YSZ plays an important role in constraining Ni coarsening in Ni-YSZ, (ii) reducing the amount of YSZ allows faster Ni coarsening, (iii) Ni-particles in a cermet with a relative high YSZ content of NiO/YSZ = 50/50 wt.% increased its average size by less than 10%, while with lower YSZ content of NiO/YSZ = 65/35 wt.% Ni-particles increased by nearly 100%. A power law model showed good fit with the experimental data with higher Ni diffusivity in the 65:35 wt.% sample, due to reduced constraint by the reduced amount of YSZ, could quantitatively explain the increased Ni coarsening.

Sehested et al [20] studied Ni catalyst sintering on spinel (MgAl$_2$O$_4$) catalyst support operating in the temperature range of 500–550°C. They assume that the Ni migration mechanism is PMC. Density functional theory calculations indicated that the NiOH species dominates Ni transport on Ni particle surfaces in steam and hydrogen containing atmospheres, because NiOH has the lowest combined energies of formation and diffusion. An expression for the diffusion constant for semi-spherical Ni-particles, D_p, was established as

$$D_p = a(d_{Ni,a}/d_p)^4 D_{NiOH} \cdot K_{NiOH} \left(pH_2O/pH_2^{0.5}\right) \quad (1)$$

where the shape dependent constant, a = 3.0, $d_{Ni,a}$ is the diameter of a Ni atom, d_p is the diameter of the Ni particle, D_{NiOH} is the surface diffusion constant for NiOH on the Ni-particle surface, pH_2O and pH_2 are partial pressures of steam and hydrogen, respectively.

K_{NiOH} is the equilibrium constant for the chemical reaction

$$Ni\,(bulk) + H_2O + Empty - site_{Ni(111)} \rightleftharpoons NiOH_{Ni(111)} + 0.5\,H_2 \tag{2}$$
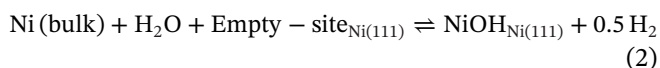
$K_{NiOH} = (pH_2^{0.5} \cdot \theta_{NiOH})/(pH_2O \cdot \theta_*)$, where θ_{NiOH} and θ_* are the coverage of NiOH and free sites on the Ni surface, respectively.

The relation between experimental catalyst sintering data and the effective mass diffusion constant for NiOH was established by numerical modeling of the particle migration and coalescence process. Using this relation, the effective mass diffusion constant as a function of temperature is determined from experimental data to

$$D_{NiOH} \cdot K_{NiOH} = 7.7 \cdot 10^{-6} m^2 s^{-1} bar^{-0.5} \exp((-137 kJ\,mol^{-1})/RT) \tag{3}$$

Even though the values of D_{NiOH} and K_{NiOH} were not determined, but only their product, the effective mass diffusion constant, Sehested's and coworkers' modeling described the experimental data well [20].

2.2 | Migration of Ni in polarized cermets in SOC

Gubner et al [2] observed that loss of nickel could explain increase in ohmic resistance as well as an increase in anode polarization during SOFC tests of 1000 to 2000 h at 950°C. Evaporation of Ni caused loss of electronic and electrochemical contacts between Ni-Ni particles and Ni-YSZ particles. It was found that the nickel loss from the cermet was independent of current density. Ni loss was also observed from stripes of anode cermets put on both sides of stripes of YSZ electrolyte and exposed over some 100 h to a flow of a mixture of methane and water vapor (1:2) at 950°C. The stripes were mounted in glass pipes. After the tests, the glass pipes showed a dark deposit of Ni (identified by EDS) in the regions where the gas cooled down. This work was taken as a clear evidence of Ni evaporation. Thus, at 950°C in SOFC test, Ni(OH)$_2$ in gas phase migrates down the pH$_2$O gradient created by the fuel oxidation in the Ni-cermet electrode. The pH$_2$O gradient is directly related to the gradient in oxygen partial pressure, pO$_2$, in cases where the atmosphere consists of only H$_2$O and H$_2$. Hagen et al [21] reported a loss of ca. 40% of Ni from a Ni-YSZ cermet electrode in a local area of about 1 cm^2 of a 16 cm^2 cell, which was tested with 1.94 A cm^{-2} at 850°C for 1500 h, and they mention that this might be due to Ni(OH)$_2$ evaporation in similarity with the findings by Gubner et al. [2]. Barfod et al [22] found that the average Ni content decreased from 26% to 19% on an anode cross section of a cell tested
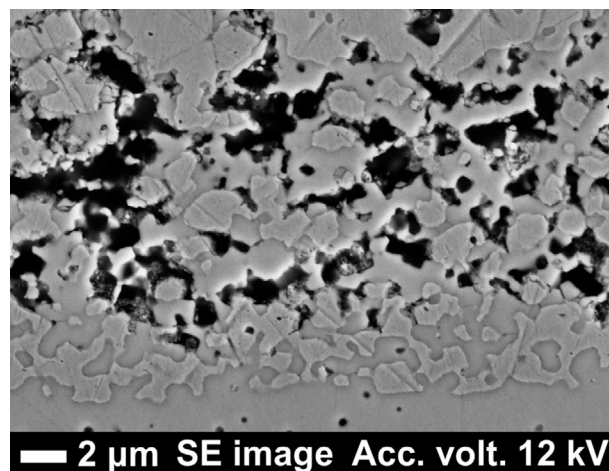
FIGURE 1 SEM micrograph of the YSZ electrolyte (bottom)/Ni-YSZ electrode, from a cell tested at 950°C for 68 h [24]. The Ni phase looks like "standing out" of the figure and has many grinding scratches from the sample preparation as Ni is soft compared to YSZ. Note the almost pore free 2–4 μm thick layer of Ni-YSZ next to the dense electrolyte

for 1000 h at 850°C in a 50/50 steam/hydrogen gas-mixture. In both these studies the Ni content was evaluated by EDS on electrode cross sections investigated prior to and after aging, meaning that above fractions are area fractions.

Menzler et al [23] recently reported on posttest characterization of an SOFC stack tested 100,000 h at 700°C and 0.5 A cm^{-2}. A surprising enrichment of Ni was observed in the Ni-YSZ cermet anode near the YSZ electrolyte. The Ni content in the pristine anode was 32 vol.%, and 40 vol.% (mean values of 10 examined micrographs) was measured after the test. Note that this is apparently a migration up the pH$_2$O gradient, which needs some more explanation, see section 3.2.

Hauch et al [24] tested an SOEC at 950°C, pH$_2$O/H$_2$ = 0.9 atm/0.1atm, −2.0 A/cm^2 for 68 h. In spite of the short-test duration, the Ni-YSZ cermet showed a significant migration of Ni into the porosities, blocking all pores of the Ni-YSZ cermet in a 2–4 μm thick layer next to the electrolyte as illustrated in Figure 1. The high level of porosity in the Ni-YSZ cermet originates in part from the Ni, which migrated away and into the original porosities next to the electrolyte. Note that in this case, the migration of Ni is again down the H$_2$O (pO$_2$) gradient created by electrolysis as expected, and this is irrespective of whether Ni(OH)$_x$ is migrating in gas phase or adsorbed on the solid electrode surface.

At temperatures below about 900°C in SOEC mode, Ni is observed to migrate away from the electrolyte, which apparently is up the pH$_2$O (and pO$_2$) gradient and the electrical potential gradient in the YSZ phase of the cermet. Tao et al [25] tested Ni-YSZ electrodes in cells at −2.0 A cm^2,
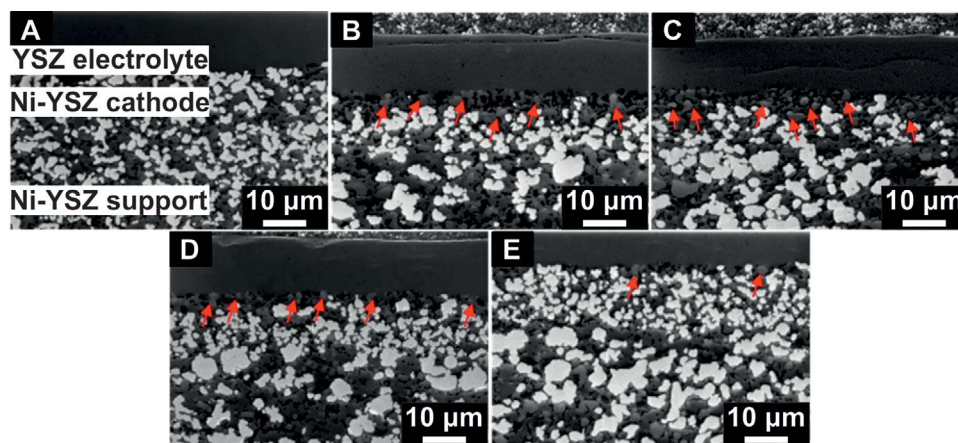
FIGURE 2 Low-voltage SEM micrographs of fine-structured Ni-8YSZ active electrode between the coarse Ni/YSZ support and the 8YSZ electrolyte. (a) pristine, and (b–e) after galvanostatic test at -2.0 A cm^{-2}, inlet gas: 45% H_2O + 45% CO_2 +10% H_2, 60% (H_2O + CO_2) conversion, temperature: 865 °C increasing to 875 °C. (b) H_2O-CO_2-H_2 inlet and (c) outlet tested 678 h, (d) inlet and (e) outlet tested 138 h. Bright colored particles: interconnected Ni; light grey: uncontacted Ni; dark grey: YSZ; black: pores. Red arrows point to uncontacted Ni. The cell voltage of the 678 h test was below 2.0 V and the 138 h test below 1.8 V. From Tao et al [25] with permission from Elsevier
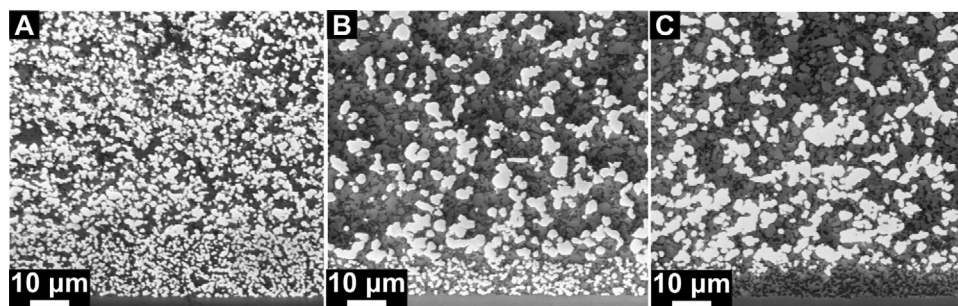

FIGURE 3 Representative LV-SEM micrographs from Ni–YSZ electrodes. (A) A pristine electrode of the same type as the electrodes in (B and C), but not from the same cell batch, and the fine-structured active electrode layer is thicker in (A). (B and C) are from the very same cell tested for 9000 h at 800°C applying an inlet gas composition of 90% H_2O + 10% H_2. (B) A part of the cell with no current load (inlet edge of the cell without oxygen electrode that is, no current load). (C) Piece of cell tested at -1 A cm^{-2} (a piece from the steam inlet part of the cell with oxygen electrode i.e., under current load). The ca. 10 µm layer with the fine Ni particles next to the electrolyte at the bottom is the active fuel electrode in all three micrographs. From [26]

inlet gas: 45% H_2O + 45% CO_2 + 10% H_2, 60% (H_2O + CO_2) conversion. One cell was tested at temperature of 865 °C increasing to 875 °C during 678 h of test, and another nominally identical cell was tested during 138 h.

Figure 2 shows a series of SEM micrographs of one not-degradation-tested (Figure 2a) and two long-term tested Ni-YSZ active SOEC electrodes. The four features seen are: (i) the white particles, which are electrically interconnected Ni particles with contact to ground in the SEM, (ii) the light gray particles are Ni particles that have lost contact to each other, (iii) the dark gray particles are YSZ, and the black features are porosity. Comparison of the tested electrodes reveals that Ni migration away from the electrolyte took place in all of the micrographs (Figure 2b–e) most at the gas inlet of the 678 h tested cell and least at the

fuel outlet of the 138 h tested cell. As both steam partial pressure and electrode overpotential are highest at the gas inlet, these results tell that the Ni migration in these cells progresses with time during periods longer than 138 h and that the migration rate increases with overpotential and pH_2O. The latter two parameters are closely related in this most electrochemically active part of the cermet electrode in both electrolysis and in fuel cell mode. Thus, Figure 2 reveals that the migration of Ni is driven by overpotential and pH_2O (pO_2).

Figure 3 shows three LV-SEM micrographs of Ni–YSZ electrodes and Ni–YSZ cell support layers [26]. Figure 3a shows a pristine electrode of the same type but not the same batch as the electrodes in Figure 3b,c, which are from the very same cell tested for 9000 h at 800°C. (B) is from a
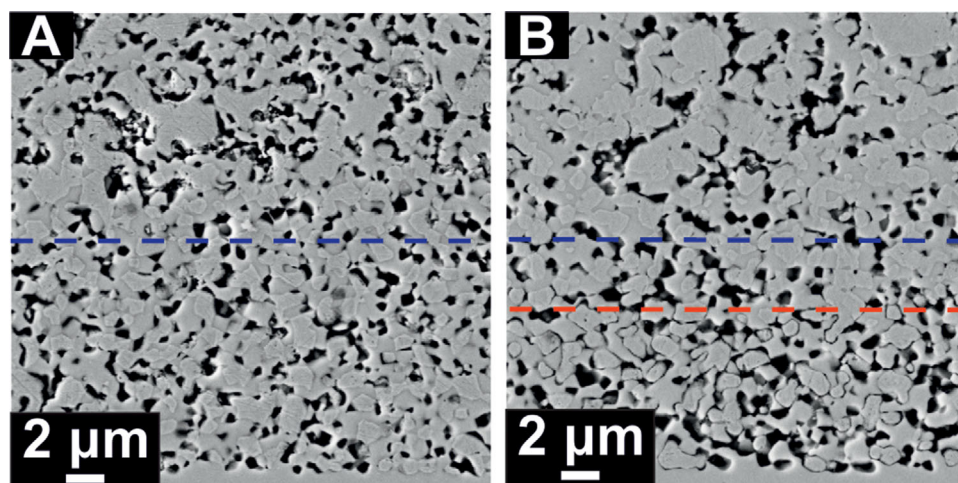
FIGURE 4 SEM micrographs of Ni–YSZ electrodes. (a) Micrograph of the pristine Ni–YSZ electrode of a reference cell (not long-term tested, only reduced and initially characterized) [28]. (b) Micrograph of a sister cell to A), but tested for 1,000 h at −1.25 A cm⁻², 90% H₂O in inlet, 56% conversion and 800°C [27]. The Figure is reproduced by permission of Elsevier. The blue dashed line indicates the border between the active fuel electrode (Ni/8YSZ) and the support layer (Ni/3YSZ) while the red dashed line in (b) guides the eye to the part of the fuel electrode, where the majority of the Ni particles have lost contact to the YSZ, which is evidenced by the crevices (black rim) around the Ni particles. Note also the increased porosity next to the dense YSZ electrolyte in the bottom of (b)

part of the cell without any oxygen electrode on the opposite side due to masking and placement of a gas sealing, and C) is from the ordinary inlet part of the Ni-YSZ electrode. Thus, the only difference between B) and C) is the polarization, that is, zero current at (B) position and -1 A cm^{-2} at (C). Note, that the part of the fine Ni in the area next to the electrolyte in (C) has been almost emptied for Ni-particles, whereas the active electrode in (B) is still intact after 9000 h at open circuit voltage (OCV). Thus, it is very clear that the electrode polarization is the totally dominating factor for the Ni migration away from the electrolyte. The rather high steam partial pressure had only a very small coarsening effect on the Ni-particles in the relatively dense active electrode. Evidently, the coarsening in the coarser and more porous support is much more pronounced. This illustrates how the zirconia constrains the Ni coarsening.

Two cells were tested with -1 A cm^{-2} and -1.25 A cm^{-2} for 2000 and 1000 h, respectively, at 800°C, p(H$_2$O)/p(H$_2$):90/10 and 56% steam conversion by Hauch et al. [27,28]. The results indicated a fuel electrode overpotential "threshold" for breakage of the interconnected Ni-network between 160 mV and 300 mV. Determining the critical fuel electrode overpotential for onset of this irreversible Ni/YSZ degradation may be used to optimize operation conditions in terms of temperature, gas composition, steam conversion and current density. The structure of the Ni-YSZ cermet is of major importance. A very fine-structured and dense structure (with only the porosity formed by the reduction of NiO at cell start) gives the most stable electrolysis cell cathode as this will have the lowest overpoten-

tial (and the most effective zirconia backbone to constrain the Ni).

Figure 4 shows another important result from the same study, namely that most Ni-particles in the strongly negative polarized part of the cermet next to the dense electrolyte have lost contact to the YSZ porous matrix. This is usually seen in tests in our laboratory and has also been observed by others. The loss of contact is very important as this means local loss of electrochemistry and will affect the electrical and electrochemical potential gradients as well as the pH$_2$O gradients in this area. If loss of electrical contact between Ni and YSZ particles happens before the start of the Ni migration then the Ni migration will also in this case be a migration down to the most negatively polarized Ni particles [26] as explained in more details below. Some researchers report that they do not see these crevices, but here we should bear in mind that it only takes a crevice of few Å width to break the contact between the particles. Furthermore, a lot of Ni-Ni loss of contact of the type revealed in Figure 3 is usually observed in long-term SOC tests, and this will also result in a very inhomogeneous electrochemical potential in this area.

This SOEC degradation phenomenon has now been studied by many research groups [3,15,29–38] as this seems to be a general, serious problem for SOEC durability. In many cases, the degradation related to Ni migration continues with an unacceptably high rate over several hundreds of hours, and the overall conclusion from all these studies is that the Ni migration may continue over several thousands of hours, fortunately with a decreasing rate, which in many cases almost stops after a few

thousand hours. In a paper that reports a 9000 h SOEC test at 775–782°C and −1 A cm^{-2}, The et al [3] state: "The most severe performance loss of the cell is caused by depletion of nickel in the cathode followed by an agglomeration in the inner part. Consequently, the electrolyte grows with nickel depletion, and the electrochemical active 3PB area is reduced. Calculations for a depleted zone of 10 μm yields a high ohmic overpotential of η_{ohm} = 0.17 V for a current density of −1 A cm^{-2}".

Trini et al [15] investigated two nominally identical SOCs with fine-structured (∼9 μm thick, average Ni particle size ∼500 nm) fuel electrodes in SOCs in both fuel cell and electrolysis cell mode at 800°C for 1000 h, inlet gas with pH$_2$O/pH$_2$ = 0.5/0.5, 1 atm, 1 A cm^{-2} and −1 A cm^{-2}. The cell degraded 10 times more in electrolysis mode than in fuel cell mode. In both cases a coarsening of the Ni particles were seen, more or less, to the same degree. The loss in percolating 3PB was much stronger in electrolysis mode than in fuel cell mode, 3PBL decreasing from 2.19 +/− 0.15 μm μm^{-3} for a pristine cell to 2.09 +/− 0.15 μm μm^{-3} in SOFC mode and to 1.36 +/− 0.15 μm μm^{-3} in SOEC mode. Moreover, a significant depletion of Ni was observed in the 5 μm thick active SOEC electrode. This was not observed in the SOFC electrode. The Ni/(Ni + Zr + Y) atomic ratio decreases in the SOEC case from ∼0.49 in the pristine cell to ∼0.28 in the cell aged in SOEC-mode, and the porosity in the same region increased from ca. 22% to ca. 33%. The authors related the differences in Ni redistribution between the two cases to a postulated polarization dependence of the Ni/YSZ interface energy (wetting angle) [39].

The migration data may be summarized as follows:

(i) At current density lower than numerical 0.25 A cm^{-2} (low overpotential) Ni does not seem to migrate over periods up to a few thousand hours.

(ii) At high current density, more than numerical 0.5–1.0 cm^{-2}, various migration processes take place.

(iii) In SOFC mode and in SOEC mode at 950°C, Ni migrates down the pH$_2$O/pH$_2$ ratio gradient, which in this context is the same as Ni migration down the electrochemical potential/pO$_2$ gradient.

(iv) In SOEC mode at lower temperatures and under strong polarization, there is a pronounced Ni migration effect away from the electrolyte, which apparently is up the electrochemical potential/pO$_2$ gradient.

(v) A fuel electrode overpotential threshold between ∼160 and ∼300 mV was observed for the breakage of the contact between Ni particles and YSZ.

(vi) In SOFC mode over a 10 year period at 700°C, Ni migrates toward the electrolyte, which again apparently is up the electrochemical potential/pO$_2$ gradient.

2.3 | Model electrodes

Using model electrodes with microns thin planar Ni patterns on planar YSZ surfaces Jiao et al [9, 39] studied the Ni migration as function of potential. They found fast migration of solid Ni (up to about 5 μm during the first hour) on top of a planar YSZ electrolyte away from a 0.5 V anodic polarized YSZ-Ni-H$_2$ 3PB in a model electrode at ca. 850°C. This Ni migration was down the electrical potential in similarity with the behavior of the anodic polarized Ni-YSZ cermet in SOFC mode and cathodic polarized Ni-YSZ at 950°C described above [2,24]. This behavior was previously reported by other researchers, who used point Ni electrodes on YSZ pellets, for example, [40,41]. Furthermore, Jiao et al [39] found that the interface free energy between Ni and YSZ was positive under cathodic polarization, that is, Ni detached spontaneously, whereas the interface energy became more negative the more the interface was anodically polarized, that is, stronger attachment with increasing anodic polarization.

2.4 | Effect of impurities

An overlooked aspect in almost all articles about Ni migration in Ni-YSZ cermets and on YSZ is that YSZ surfaces and grain boundaries as well as Ni-YSZ interfaces almost always have thin monolayers of impurities or of segregated components. This is extremely difficult to avoid since trace impurities tend to segregate to surfaces and interfaces, and it takes dedicated surface science techniques such as XPS or TOF-SIMS in order to observe such thin films [42]. YSZ raw materials that are regarded as pure may contain relatively high levels of S and Cl. In a batch of 8YSZ, a content of 200 ± 15 ppm S and 5700 ± 200 ppm Cl was measured by glow discharge mass spectrometry [43].

Likewise, trace impurities in a gas stream containing CO$_2$ and CO can, within a few hundred hours of SOEC testing, lead to detrimental damage of the network properties for the Ni-YSZ cermet electrodes due to Ni migration, as reported in [44] where this subsequently led to carbon deposition. Studies following this work showed that it was gas stream sulfur-based impurities in quantities of 15–20 ppb in the CO$_2$ feed for the CO$_2$ electrolysis that initiated the severe degradation. Also silica is often observed, and for example Riedel et al [45] used ultrapure water with a Si concentration of 4 to 7 μg L^{-1} for steam raising for an SOEC stack test over 1000 h and found an average of ca. 2.3 wt.% Si across the fuel electrode thickness at the inlet and spots with up to 5.5 wt.% Si close to the electrode-electrolyte interface. Notice that Si species will be transported in the gas phase mainly as Si(OH)$_4$. Upon steam electrolysis the equilibrium between Si(OH)$_4$ and silica

(SiO_2) will be shifted toward SiO_2 due to the consumption of H_2O in the electrolysis process. This in turn will lead to SiO_2 forming at the 3PB during H_2O electrolysis, while this will not occur during SOFC operation of the SOC.

2.5 | Data about alleviation of Ni migration problems

Fortunately, several methods to mitigate the Ni migration problems have been reported. Hauch et al [44] observed that Ni migration in the active Ni-YSZ electrode layer is aggravated by gas impurities in case of electrolysis of dry CO_2. This indicates that proper steam and gas cleaning may alleviate the observed degradation and can be an important factor in maintaining the desired Ni-YSZ and Ni-Ni network properties. Possibly, cleaning of the cell raw materials will also help.

Infiltration or other ways of adding a mixed ion and electron conductor like Gd_2O_3 doped CeO_2 (CGO) as nanoparticles to the Ni-YSZ-electrode seem to alleviate the Ni migration related to SOEC electrode degradation [37,46]. CGO is a mixed ionic and electronic conductor (MIEC) in reducing atmosphere and decreases the polarization resistance of the Ni-YSZ 3PBs, which in turn decreases the overvoltage of the electrode. By infiltrating CGO nanoparticles into the Ni-YSZ electrode, Ovtar et al [46] reduced the cell voltage degradation rate from 699 mV kh^{-1} for the bare Ni-YSZ electrode to 66 mV kh^{-1} for the infiltrated electrode at a current density of -1.25 A cm^{-2} at 800°C. Even after significant degradation, it is possible to reactivate cells by infiltrating Ni-YSZ cermet of the cell with CGO [47], and re-activation of degraded Ni-YSZ cermet fuel electrode is possible by subjecting it to reverse current pulses that form zirconia nano-particles [48].

Instead of infiltration of CGO nanoparticles, YSZ may be substituted with CGO in the active fuel electrode, that is, use a Ni-CGO composite, in order to broaden the 3PBs as much as possible. An electrolyte supported SOEC with such a fuel electrode was operated during 23,000 h in the steam electrolysis mode, of which 20,000 h were with -0.9 A cm^{-2} at 850°C. The Ni-CGO electrode had no visible damage of the H_2 electrode after testing [49]. Uchida et al [50] examined durability of a double-layer fuel electrode, which consisted of a samaria-doped ceria scaffold with dispersed ca. 7 vol.% $Ni_{0.9}Co_{0.1}$ + 10 vol.% Ni nanoparticles as catalyst layer. A 200 mesh (74 μm spacing) Ni, 0.1 mm thick wires, acted as current collector. Tests of fuel electrodes in both SOFC and SOEC at 800°C were carried out in a continuous constant current density mode at -0.50 A cm^{-2} and in a reversible cycling mode between -0.50 A cm^{-2} SOEC mode for 11 h and 0.50 A cm^{-2} SOFC mode for 11 h with a current sweep rate of ± 1.00 A cm^{-2} h^{-1}

between the two modes (24 h cycle^{-1}). Continuous SOEC mode resulted in a rapid, large increase in the ohmic resistance on the hydrogen electrode side, whereas the reversible cycling operation between SOEC and SOFC modes had almost no degradation over 1200 h. This could be ascribed to a stabilization of the microstructure of the hydrogen electrode. In terms of showing a positive effect of cycling, these findings are similar to the findings by Graves et al [51], who demonstrated on a Ni-YSZ cermet-based SOC that severe electrolysis-induced degradation, which was previously believed to be irreversible, can be completely eliminated by reversibly cycling between electrolysis and fuel-cell modes. Continuous SOEC mode at -1A cm^{-2}, initially at 1.33V, led to a large increase in ohmic resistance, while after 4000 h of reversible cycling, the ohmic resistance was slightly improved. Inspired by this, Jensen et al [52] recently proposed to use a novel scheme for powering of SOEC with a kind of alternating current with an overlay of SOFC mode for few milliseconds with a frequency of for example 30 Hz. This so-called AC:DC powering scheme also seems to impede the SOEC degradation.

Addition of a Ni-YSZ wetting agent that makes the interface free energy more negative is also a possibility. This is probably what happens by addition of Al and Ti in the form of Al_2TiO_5, which Law and Sofie [53] and Driscoll et al [54] used to "anchor" Ni-particles to the YSZ to prevent coarsening and migration of Ni particles. Infiltration with aluminum titanate increased Ni catalyst stability in Ni-YSZ electrode such that "the time required for degradation to 90% of initial current output was increased by a factor of 115" [54].

The ultimate way to circumvent the degradation problems related to Ni migration is to replace the Ni with another electron conducting catalytic material. Such materials have been researched for many years [55]. This may be a single phase MIEC oxide materials, which provide electrochemical reaction sites on the entire surface/gas two-phase boundary (2PB), and making them less susceptible to blockage by impurities than 3PB-based electrodes. Alternatively, it may be a mixture of MIEC and an electron conductor. CGO is an MIEC and very promising as an electrocatalytic component of a composite electrode where another material provides sufficient electronic conductivity [56,57].

## 3 | MECHANISM HYPOTHESIS

3.1 | Literature considerations

A striking feature of the literature data is that both in SOFC and SOEC mode the Ni migrates down the pH_2O gradient at 950°C and perhaps to some extent at 850°C as

expected if a $Ni(OH)_x$ species is involved in the migration, whereas at 700°C for SOFC and at 850°C and below for SOEC, Ni apparently migrates up the pH_2O gradient. This SOEC case was explained qualitative by us previously by migration of $Ni(OH)_x$ either in gas phase [25,26] or adsorbed on the solid Ni and YSZ surfaces. Many of the listed references reject the gas-phase transport possibility because of the low calculated partial pressure and the electrode potential dependence. For example, Menzler et al [35] wrote "Mogensen et al stated that polarization plays a key role but did not provide a value at which migration occurs. Transport occurs by Ni evaporation, for example $Ni(OH)_x$, but internal calculations of the evaporation pressures under the operation conditions did not support this assumption" with reference to [26]. A clear example of the important effect of potential is given in Figures 2 and 3, and numbers are given for the overpotential threshold for onset of Ni migration in DTU type SOC at given conditions. With respect to migration of Ni in gas phase, probably as $Ni(OH)_2$, a very clear evidence was reported by Gubner et al. [2]. However, we agree that Ni probably does not migrate much as a gaseous compound below 800°C, because the partial pressure of Ni and Ni-H_2O reaction compounds are very low under all SOC cermet electrode working conditions at 800°C and below as illustrated in Figure 5. We hypothesize that the Ni migration at temperatures below 800°C in both SOFC and SOEC mode takes place by surface diffusion in analogy to Sehested's model for Ni migration as NiOH on the surface of Ni catalyst supported by $MgAlO_4$ [20] as described in section 2.1.

Some researches seem to be of the opinion that electrochemistry is not involved in Ni migration. As an example, Chen et al [58] state that "Ni coarsening in the SOFC anode is a capillarity-driven phenomenon. Regions with high curvatures have higher chemical potentials than those with lower curvatures in accordance with the Gibbs-Thompson effect: the increase in free energy due to curvature, and thus the material will be transported from these regions to lower-curvature regions when mobility is sufficiently large for the time scale of interest. This leads to lower free energy of the system." We do not agree fully in this. The first sentence is correct if it is taken into account that electrochemical polarization will also affect the surface and interface energy. However, the Ni-YSZ cermets do probably not follow the Gibbs-Thomson equation as this describes gas bubble formation in liquids or particle growth of solid homogeneous particles in a liquid in which the particle material has some solubility.

Many researchers in the area have tried to model the migration by phase-field modeling with varying success. Lei et al [59] developed a phase-field model to simulate Ni particle growth and redistribution through formation and diffusion of gaseous $Ni(OH)_2$. Their basic assumption
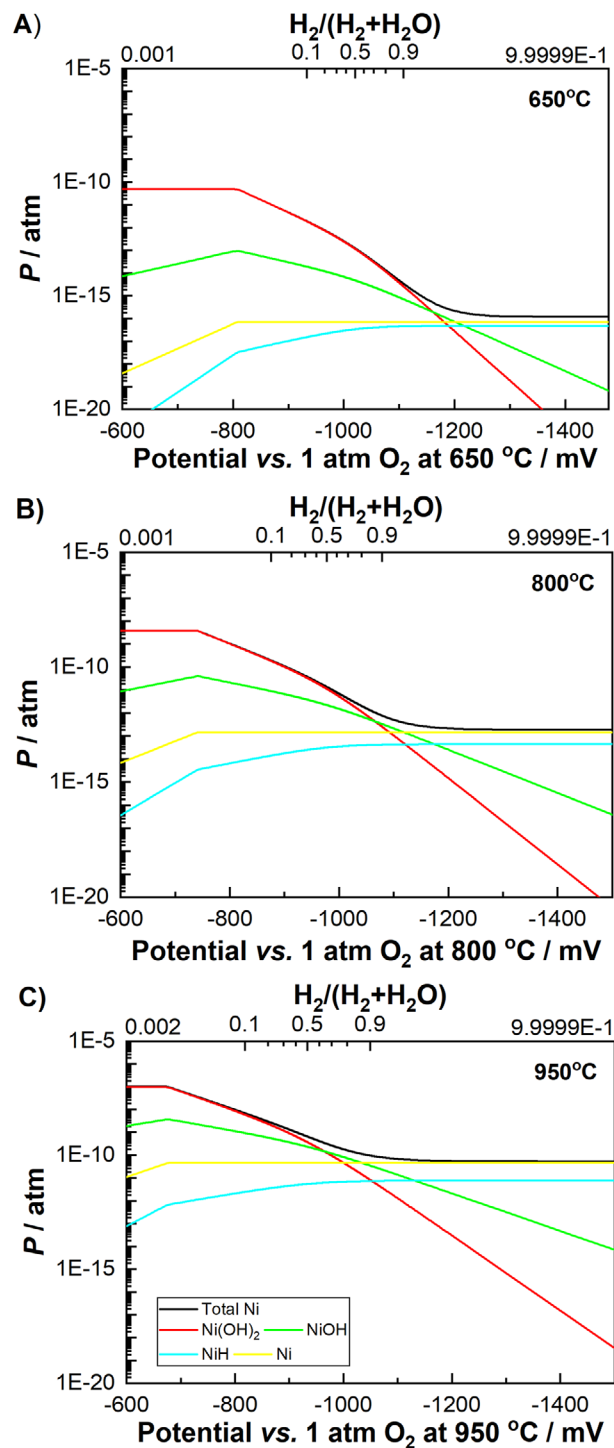
FIGURE 5   Total and partial pressure of Ni gas species over solid Ni electrode in hydrogen–steam mixtures as function of Ni electrode potential versus 1 atm oxygen and the equivalent ratio $p(H_2)/(pH_2 + pH_2O)$ at three different temperatures, (a) 650°C, (b) 800°C, and (c) 950°C. The calculations were carried out using FactSage® Thermochemical Software and Databases [61]

was that Ni(OH)$_2$ diffusion would be in the direction of the pH$_2$O gradient, and their conclusion was:

(i) Ni(OH)$_2$ diffusion does not affect the coarsening rate due to its small mass flux, but it leads Ni to migrate away from the electrolyte layer in the fuel cell mode and to the electrolyte layer in the electrolysis mode.

(ii) Ni-YSZ wettability change affects the coarsening rate by changing the Ni-YSZ contact angle, but it has no significant effect on Ni redistribution under current model.

(iii) None of the mechanisms are able to fully explain the experiments.

Nakajo et al [60] tried to correlate variation in dihedral angle with potential and Ni particle migration with some success, but they leave a Ni migration mechanism via gas phase open.

Previously, we have hypothesized that the migration of Ni away from the YSZ|Ni-YSZ- electrolyte|electrode interface was caused by (i) loss of contact between Ni- and YSZ-particles in the volume of the Ni-YSZ cermet next to the electrolyte, followed by (ii) NiOH migration toward the new 3PBs with lowest electrical potential formed just outside the layer with loss of Ni-YSZ particle contact [26]. The next section provides a revised hypothesis for Ni migration in Ni-YSZ cermet electrodes.

3.2 | Revised and extended hypothesis

The hypothesis of this article is a mechanism that qualitatively can explain that Ni particle migration in real cells goes via the formation of surface and/or gas phase species of Ni(OH)$_x$, x = 1 or 2, according to Equation (4), electrochemistry, or Equation (5), chemistry only:

$$Ni(OH)_x\,(g) + 2x\,e^-\,(Ni) \rightleftharpoons Ni\,(s) + x\,O^{2-}\,(YSZ) + \tfrac{1}{2}x\,H_2\,(g) \tag{4}$$

$$Ni(OH)_x\,(g) + \tfrac{1}{2}x\,H_2\,(g) \rightleftharpoons Ni\,(s) + x\,H_2O\,(g) \tag{5}$$
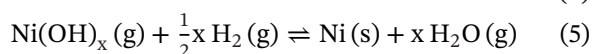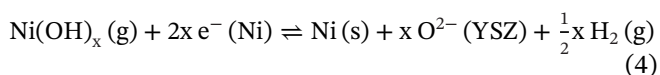
Figure 5 shows calculated total and partial pressure of Ni gas species, Ni, NiH, NiOH, and Ni(OH)$_2$ over solid flat Ni electrode in hydrogen-steam mixtures as function of electrode potential versus 1 atm oxygen and the equivalent ratio p(H$_2$)/(pH$_2$ + pH$_2$O) at three different temperatures, 650°C, 800°C, and 950°C [61]. It reveals that under relatively reducing conditions x may be 1 and under more oxidizing conditions x may be 2, that is, x = 1 is dominating in SOEC mode with strongly negative polarization (equivalent to high pH$_2$/(pH$_2$ + pH$_2$O)), and x = 2 in SOFC mode with strongly positive polarization (equivalent to low pH$_2$/(pH$_2$ + pH$_2$O)). Under strongly reducing conditions,

Ni metal has the highest calculated partial pressure. Here, it is noted that as soon as an Ni particle is not in contact with the polarized Ni cathode then the potential of the Ni will be much more positive due to the general high steam content in the gas phase around the active Ni-cermet electrode both in SOEC cathode as well as in SOFC anode. A gas with less than 1% H$_2$O, that is, H$_2$/(H$_2$+H$_2$O) higher than 0.99, will not appear in a practical working SOEC outside the surface of the strongly negatively polarized Ni.

The activity, a_i, of a gas species, i, is $a_i = \gamma_i(P_i/P°)$ and the chemical potential, μ_i, of species i is $\mu_i = RT\,ln(a_i)$. γ_i is the activity coefficient of species i, P_i the partial pressure of species i, and $P°$ is a reference partial pressure. Furthermore, at equilibrium between gas phase and Ni-surface, $\mu_{Ni(OH)x,gas} = \mu_{Ni(OH)x,surface}$. Even though equilibrium may not be reached in all steps, this means that whether it is gas diffusion or particle migration at 500°C as proposed by Sehested, the driving forces will be the same, but the kinetics may naturally be different.

An attempt to explain the apparent Ni migration against the potential and pO$_2$ gradients is given in the following. Figure 6 depicts two snapshots of degrading Ni-YSZ electrodes, one in SOEC, the other one in SOFC mode after a significant duration of operation at high overvoltage. In the SOEC case, the overvoltage was from the beginning numerically above the threshold for Ni-YSZ particle contact breakage in the 3PB. Breakage of contact between Ni and YSZ means no further electrochemistry, and the Ni particles will obtain the pO$_2$ potential of the local gas. In an SOFC case, a somewhat lower overvoltage than for SOEC will be used in most cases, and there is no sharp onset potential threshold as Ni-YSZ adhere well to each other. However, over very long time period, a significant amount of Ni particles will lose the connection to other connected Ni particles because of Ni particle coarsening. And again, an electronically insolated Ni particle will obtain the potential of the pO$_2$ potential of the surrounding H$_2$O-H$_2$ gas mixture.

We imagine that the cross-sections pass exactly through most polarized Ni particles in the narrow new 3PB zones that formed after the detachment of Ni particles from YSZ near the dense electrolyte. A vertical dotted line in each cross-section indicates the position of the most electrochemically active Ni particles. Further, there is electrical contact between all YSZ particles and the dense YSZ electrolyte at any time. We imagine that the cross-sections are close to the steam and oxygen inlet of cathode and anode, respectively.

The curves in Figure 6 depict qualitatively the variations of three important parameters, η, the local overvoltage of Ni particles, pH$_2$O, steam partial pressure, and $a_{Ni(OH)x}$, the activity of Ni(OH)$_x$ species versus distance from the surface ($d = 0$) of the dense YSZ electrolyte. It should be

SOEC cathode

SOFC anode
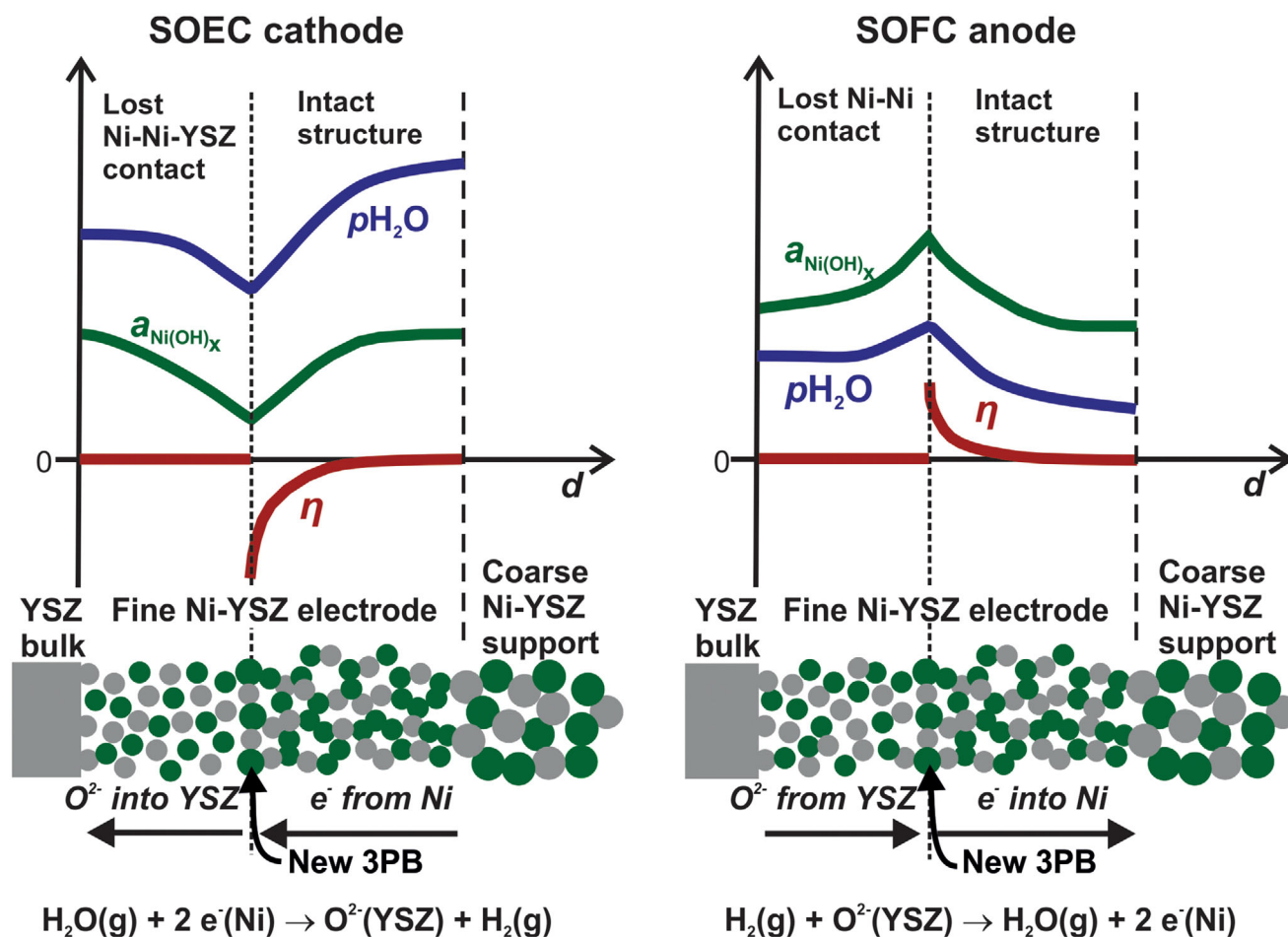
FIGURE 6 Sketches of cross-sections of degrading Ni-YSZ cermet electrodes in SOEC mode (left) and SOFC mode (right). Green depicts Ni and gray YSZ. Contacts between Ni-YSZ and Ni-Ni particles have been lost in the initial active 3PB zones next to the bulk YSZ electrolyte. Significant Ni migration is imagined in both cases. Qualitative variations of three important parameters, η, the local overvoltage of Ni particles, pH_2O, steam partial pressure, and $a_{Ni(OH)_x}$, the activity of $Ni(OH)_x$ species versus distance from original electrolyte/electrode interface ($d = 0$) are indicated. See text for more details

noted that it is for identical Ni-YSZ electrodes, one tested in SOEC mode, that is, the cathode and the other in SOFC, that is, the anode. In the following each of the six curves are explained in details.

The effect of the overpotential, η, of Ni in <u>cathode</u> (SOEC) mode: Strong cathodic overpotential will separate the YSZ and the polarized Ni according to Jiao et al [39]. When loss of electrical contact between the Ni-Ni particles (due to Ni-particle growth) as well as between Ni-YSZ has occurred no more electrochemistry can take place, and then the Ni particles have zero overpotential. The 3PB region has then moved to the area further away from the YSZ electrolyte at d = 0 to the part where Ni still is in electrical contact with Ni in the cell support through interconnected Ni-particles. The interconnected Ni with shortest distance to the dense electrolyte then has the most negative overpotential, which fades out to zero overpotential few μm further away from the dense YSZ toward the Ni-YSZ

support due to the relatively low oxide ion conductivity of YSZ. Note that the Fermi potential of the Ni is very close to constant throughout all electrically contacted Ni, because Ni has a very high electron conductivity, and therefore only the changes in Galvani potential inside the YSZ are important. (The overpotential is the <u>change</u> (caused by polarization) in the difference between Fermi potential inside the Ni and the Galvani potential inside the YSZ).

The loss of Ni contact with loss of overpotential in the zone next to the electrolyte has two consequences: (i) the potential of the isolated Ni particles will go back to the much more positive potential of local OCV and pH_2O will be higher, because some of the steam from the steam channel will pass though the porous zone with active 3PBs without getting in contact with the polarized Ni particles, where the hydrogen evolution takes place. It is here important to imagine the real 3D situation. Some H_2O will diffuse all the way to the dense electrolyte, and H_2O will

be reduced on all sides of 3PBs. Therefore, the pH_2O will be in local minimum all around the Ni particles with active 3PBs. (ii) a_{NiOH} will naturally follow η and be lowest where η is lowest at the very reducing 3PB line (dotted vertical line) with the consequence that Ni will precipitate via reaction (3) on the polarized Ni particles in the 3PB zone. This will happen irrespective of whether NiOH diffuses in gas phase or on the Ni and YSZ surfaces. Yet, bridging the few angstrom wide crevices between Ni and YSZ particles may take place through gas phase.

The effect of the overpotential, η, of Ni in anode (SOFC) mode: When loss of electrical contact between the Ni-Ni particles has taken place next to the electrolyte due to Ni-particle growth in the region with high pH_2O from the oxidation of H_2O then the 3PB region moves to the area further away from the dense YSZ electrolyte to the part where Ni particles still are in electrical contact with Ni in the support through interconnected Ni-particles. As Ni at OCV and more positive potentials adhere well to YSZ particles, it is only the Ni particle growth which decreases the interconnectivity between the Ni particles. During the time preceding the sketched situation, the Ni particles next to the electrolyte had the most positive potential and therefore the highest pH_2O pressure due to oxidation of H_2. The higher pH_2O will increase the Ni particle growth rate and by this increase rate of loss of contact, but this process is much slower than the process of loss of Ni-YSZ contact in SOEC mode. Late during a very long-term SOFC test, a situation as sketched in Figure 6 may be reached. The interconnected Ni with shortest distance to the dense electrolyte then has the most positive overpotential, which fades out to zero overpotential a few μm further away from the dense YSZ toward the Ni-YSZ support due to the relative low oxide ion conductivity of YSZ. The loss of Ni contact with loss of overpotential in the zone next to the electrolyte again has two consequences: (i) the potential of the isolated Ni particles will go back to the more negative potential of local OCV and pH_2O will be lower, because some of the hydrogen from the inlet will pass though the porous 3PB zone without getting in contact with the polarized Ni particles, where the hydrogen oxidation takes place. (ii) $a_{Ni(OH)}$ will naturally follow η and be highest where η is highest in the very oxidizing 3PB zone, because Ni will be oxidized via reaction (4) on the polarized Ni particles in the 3PB zone. Hence, $Ni(OH)_2$ will migrate toward the electrolyte and be converted to Ni via the reverse reaction (4).

In other words, in these situations Ni may migrate down the local pO_2 (pH_2O/pH_2) gradient in the vicinity of the active 3PB for both SOEC and SOFC modes in spite of the fact that the small pO_2 (pH_2O/pH_2) gradient in the supporting layer outside the active fine structured Ni-YSZ active electrode is opposite.

Some researchers, see for example, [15,39], argue that Ni will migrate up the pO_2 gradient, because the contact angle is the driving force for the Ni migration, and that "in SOEC mode, the electrode/electrolyte interface presents a higher contact angle compared to the region in the proximity of the gas channel." Accordingly, Ni should migrate from the active electrode toward the support layer, as observed experimentally in this work and in previous studies.

An argument against this is that it is clear from Figure 2 that a lot of not-interconnected (non-percolating) fine Ni-particles are present in the active electrode layer during the first several hundreds of hours, and in Figure 3 after 9000 h almost all small Ni-particles have been removed by the polarization. As the non-interconnected Ni particles are not polarized they are exposed to a much higher pO_2 than the interconnected ones. This implies that these non-polarized Ni-particles (with an electrical potential close to OCV) should grow and not disappear according to the hypothesis in [15] if this was the only mechanism of transport. Also, Jiao et al observe that Ni does not migrate away from cathodically polarized Ni-YSZ 3PB in their model electrodes [39], while Ni migrates away from an anodically polarized Ni-YSZ 3PB as predicted by the present hypothesis.

Another point is that whether a contact angle gradient (interface energy gradient) will be the driving force or other possible mechanisms like gradients in redox potential will be strongest, must depend on the mechanism and the overall process. In the Ni-YSZ cermets it looks as if the migrating Ni does not move to other places on the YSZ, but rather moves onto already existing polarized Ni-particles. And clearly, Ni-metal will be the more stable, the lower the pO_2 is.

As reported by Hauch et al [44], Ni-migration may also happen in dry CO_2-CO atmosphere. This might be taken as an argument against the hypothesis presented above, but there is no reason to believe that Ni migration cannot take place via mechanisms different from the $Ni(OH)_x$-transport, for example, it is not difficult to imagine a PMC migration mechanism based on Ni-O-species or Ni-impurity-species. More work is definitely needed in order to figure out, which species are responsible for Ni particle migration in dry CO-CO_2 atmospheres. Anyway, if the Ni migrates as Ni compounds in which Ni has a positive oxidation state, x, then Ni will migrate down a possible electrochemical potential gradient to places where the Ni^{x+} will be reduced to Ni metal.

A good hypothesis needs to explain (i) why the loss of Ni-YSZ and Ni-Ni particle contact happen?, (ii) how it is it possible for Ni to migrate so fast?, (iii) why does the Ni-YSZ electrode degradation and Ni migration in SOEC with high overvoltage start with a high rate and then slow

down and asymptotically approaches zero after hundreds to thousands of hours of testing?

Regarding (i), the loss of Ni-YSZ contact in the cathode, this seems to be well explained by the spontaneous Ni detachment observed by Jiao et al [39]. It is due to the increase of Gibbs free energy of Ni-YSZ interface with increasing negative overpotential of the Ni particles.

When the interface free energy increases to above zero there is no adherence between Ni and YSZ. The Ni-Ni loss of contact happens in both cathode and anode mode due to Ni-particle growth as described in section 2.1 Also, it should be noted that the apparent Ni-YSZ interface energy may vary a lot depending on the impurities present at the interface. Often silica containing interface films are observed on YSZ. Such surface or interface films may be electrochemically reduced under SOEC conditions and thus separate Ni and YSZ particles, in similarity with the proposal by Tong et al [37] (but the Ni-YSZ electrode potential will generally not be low enough to reduce YSZ).

Regarding (ii), the migration rate of Ni is faster than we can explain by the calculated very low partial pressure of gaseous $Ni(OH)_x$ species below 850°C. Another explanation is the PMC mechanism with the Ni-particle migration driven by electrical potential and pO_2 gradients [15,39,62]. The PMC mechanism cannot, however, explain the migration over long distance of the Ni-YSZ cermet to the cold outlet of the test container [2], or the effect of the type of inert gas [4]. This raises the questions: can we think (a) of reasons for why we calculate too low partial pressures of Ni-OH species, or (b) of other gaseous Ni species that may have a higher partial pressure at SOEC operation temperature? Regarding (a), the available thermodynamic data for Ni-H_2O at temperatures above 650°C seem not very well explored experimentally, so unknown species or unknown properties cannot be ruled out. However, we can say that the vapor pressure will - everything else equal - be higher for a small particle than for a large particle, but we cannot calculate this difference without knowing the integral value of all contact angles and the surface free energy including the effect of the impurities at the surfaces and the Ni-YSZ interface. Regarding (b) combinations of Ni with impurities like sulfur or phosphor might result in more volatile compounds, such as NiSH or $NiPH_2$, but this needs to be explored.

Regarding (iii), why the Ni-YSZ SOEC electrode degradation rate starts high and then fades out over time in galvanostatic durability tests. We see three reasons for this. One is that gradually, the migrating Ni will locally fill all the pores in the YSZ structure in the zone with the new 3PBs. When this happens, Ni and YSZ will stay in contact in spite of positive interface free energy. Another possible contributing reason is that the early degradation leaves a layer of porous YSZ with unconnected Ni particles, which

gives a significant increase in the electrolyte resistance near the steam inlet in particular, and therefore the local overpotential decreases, and this again decreases the local Ni overpotential, which in turn decreases the local degradation rate. A third possible reason may be the increasing volume of Ni in the zone with new 3PBs. This may gradually stop the diffusion of steam through this zone toward the dense electrolyte, decrease the redox potential of the $H_2O + H_2$ gas and thereby decrease the electrical potential of electrically isolated Ni, and this will impede the migration rate of Ni. It will take a significant 3D modelling effort and more data to quantify the effects of these three possibilities.

3.3 | Outlook

A lot more quantitative knowledge about Ni migration on YSZ and in Ni-YSZ cermets is needed in order to be able to describe quantitatively the Ni migration processes to an extent that will make us able to predict the associated degradation rate of the SOC fuel electrode under given operation conditions. Also, the distributed local values and gradients of overpotential, potential, temperature and gas composition, pH_2O, pH_2, pCO_2, pCO, and pO_2 at the 3PBs are needed. First of all, we need to be able to reproduce the degradation, that is, to show that we can control the parameters. Next, we have to measure vapor-pressures of gaseous Ni containing species over Ni nanoparticles as a function of reactant gas composition, pressure, temperature, and electrochemical polarization. Also, surface coverage of Ni-species on Ni and on SZ (stabilized zirconia in general) should be measured. Further, it is necessary to determine free energy of Ni-SZ interfaces, of Ni and SZ surfaces, plus Ni-SZ contact angles, and the inter-dependence on the above mentioned basic parameters. It is in particular important to include tests with selected and known impurities, including trace impurities in all work mentioned above.

4 | CONCLUSION

The hypothesis in this paper is electrical potential driven Ni migration in reversible SOC fuel electrodes takes place as NiOH, $Ni(OH)_2$, as Sehested et al found in their DFT calculations [20], or as similar compound with Ni in a positive oxidation state. This implies that Ni will migrate down the electrochemical and/or pO_2 potential gradients, that is, from relative positive local potential toward relative negative potential, irrespective of whether the Ni compound is in a gaseous form at high temperatures above ca. 900°C, or in a solid adsorbed form on the Ni and YSZ surface at

temperatures below ca. 800°C. If no electrochemical or chemical redox gradients exist then the migration of Ni particle growth is a simple surface energy driven mechanism (Oswald ripening or PMC), and then there is no need for any loss of electrical contact to Ni as a pre-condition for Ni migration.

The hypothesis can qualitatively explain the reported observations. It explains how the Ni-particles apparently migrate up the electrical potential gradient due to the fact that a lot of Ni particles lose the electric contact to the surroundings, and by this obtain the oxygen potential of the local H_2O/H_2 ratio (the same as local OCV). These local potential gradients push the $Ni(OH)_x$ or similar compounds to migrate down local redox potential gradients with opposite slopes of the overall electrical potential gradient.

Another group of hypotheses in the literature assumes that it is gradient in Ni-YSZ contact angles that drives the Ni migration. Based on the present knowledge it is not possible to decide which one of the two hypotheses that provides the most proper description, and maybe future research will show that it is just two aspects of the same driving force, because interfacial energy that determines the contact angle is also strongly affected by electrode potential, a phenomenon that is called electrocapillarity. However, it should be noted that this effect of polarization on an interface with constant composition results in a fairly symmetrical decrease of Gibbs free energy of interface formation, ΔG_{if}, around the electrocapillary maximum. As this is not the case, most likely the surface tension is determined by a superposition of interfacial changes and electrocapillarity.

CONFLICT OF INTEREST
The authors declare that there is no conflict of interest that could be perceived as prejudicing the impartiality of the research reported.

ACKNOWLEDGMENTS

ORCID
Mogens B. Mogensen PhD https://orcid.org/0000-0002-0902-0580

REFERENCES
1. D. Simwonis, F. Tietz, D. Stöver, *Solid State Ion.* **2000**, *132*, 241.
2. A. Gubner, H. Landes, M. Metzger, H. Seeg, R. Stübner, *SOFC V. Proc. Electrochem. Soc.* **1997**, *40*, 844.
3. D. The, S. Grieshammer, M. Schroeder, M. Martin, M. Al Daroukh, F. Tietz, J. Schefold, A. Brisse, *J. Power Sources* **2015**, *275*, 901.
4. M. H. Pihlatie, A. Kaiser, M. Mogensen, M. Chen, *Solid State Ion.* **2011**, *189*, 82.
5. D. W. Dees, T. D. Claar, T. E. Easler, D. C. Fee, F. C. Mrazek, *J. Electrochem. Soc.* **1987**, *134*, 2141.
6. K. Thydén, Y. L. Liu, J. B. Bilde-Sørensen, *Solid State Ion.* **2008**, *178*, 1984.
7. L. Holzer, B. Iwanschitz, T. Hocker, B. Münch, M. Prestat, D. Wiedenmann, U. Vogt, P. Holtappels, J. Sfeir, A. Mai, T. Graule, *J. Power Sources* **2011**, *196*, 1279.
8. P. Tanasini, M. Cannarozzo, P. Costamagna, A. Faes, J. Van herle, A. Hessler-Wyser, C. Comninellis, *Fuel Cells* **2009**, *9*, 740.
9. Z. Jiao, N. Shikazono, N. Kasagi, *J. Electrochem. Soc.* **2012**, *159*, B285.
10. D. Kennouche, Y.-C. Karen Chen-Wiegart, J. S. Cronin, J. Wang, S. A. Barnett, *J. Electrochem. Soc.* **2013**, *160*, F1293.
11. O. M. Pecho, A. Mai, B. Münch, T. Hocker, R. J. Flatt, L. Holzer, *Materials* **2015**, *8*, 7129.
12. S. De Angelis, P. S. Jørgensen, E. H. R. Tsai, M. Holler, K. Kreka, J. R. Bowen, *J. Power Sources* **2018**, *383*, 72.
13. M. Trini, P. S. Jørgensen, A. Hauch, J. J. Bentzen, P. V. Hendriksen, M. Chen, *J. Electrochem. Soc.* **2019**, *166*, F158.
14. E. Lay-Grindler, J. Laurencin, J. Villanova, P. Cloetens, P. Bleuet, A. Mansuy, J. Mougin, G. Delette, *J. Power Sources* **2014**, *269*, 927.
15. M. Trini, A. Hauch, S. De Angelis, X. Tong, P. Vang Hendriksen, M. Chen, *J. Power Sources* **2020**, *450*, 227599.
16. G. J. Nelson, K. N. Grew, J. R. Izzo, J. J. Lombardo, W. M. Harris, A. Faes, A. Hessler-Wyser, J. Van herle, S. Wang, Y. S. Chu, A. V. Virkar, W. K. Chiu, *Acta Mater.* **2012**, *60*, 3491.
17. J. S. Cronin, J. R. Wilson, S. A. Barnett, *J. Power Sources* **2011**, *196*, 2640.
18. M. Hubert, J. Laurencin, P. Cloetens, B. Morel, D. Montinaro, F. Lefebvre-Joud, *J. Power Sources* **2018**, *397*, 240.
19. Y. K. Chen-Wiegart, D. Kennouche, J. S. Cronin, S. A. Barnett, J. Wang, *Appl. Phys. Lett.* **2016**, *108*, 083903.
20. J. Sehested, N. W. Larsen, H. Falsig, B. Hinnemann, *Catal. Today* **2014**, *228*, 22.
21. A. Hagen, R. Barfod, P. V. Hendriksen, Y.-L. Liu, S. Ramousse, *J. Electrochem. Soc.* **2006**, *153*, A1165.
22. R. Barfod, Y.-L. Liu, P. H. Larsen, P. V. Hendriksen, *Proc. Electrochem. Soc.* **2003**, *PV 2003–07*, 1158.
23. N. H. Menzler, D. Sebold, Y. J. Sohn, S. Zischke, *J. Power Sources* **2020**, *478*, 228770.
24. A. Hauch, S. D. Ebbesen, S. H. Jensen, M. Mogensen, *J. Electrochem. Soc.* **2008**, *155*, B1184.
25. Y. Tao, S. D. Ebbesen, M. B. Mogensen, *J. Power Sources* **2016**, *328*, 452.
26. M. B. Mogensen, A. Hauch, X. Sun, M. Chen, Y. Tao, S. D. Ebbesen, K. V. Hansen, P. V. Hendriksen, *Fuel Cells* **2017**, *17*, 434.
27. A. Hauch, K. Brodersen, M. Chen, M. B. Mogensen, *Solid State Ion.* **2016**, *293*, 27.
28. K. Brodersen, A. Hauch, M. Chen, J. Hjelm, *European Patent Application No 1518138.3*, **2015**.
29. M. Chen, Y.-L. Liu, J. J. Bentzen, W. Zhang, X. Sun, A. Hauch, Y. Tao, J. R. Bowen, P. V. Hendriksen, *J. Electrochem. Soc.* **2013**, *160*, F883.
30. Y. Yan, Q. Fang, L. Blum, W. Lehnert, *Electrochim. Acta* **2017**, *258*, 1254.

31. E. Hernandez, F. Baiutti, A. Morata, M. Torrell, A. Tarancon, *J. Mater. Chem. A* **2018**, *6*, 9699.

32. M. Riegraf, A. Zekri, M. Knipper, R. Costa, G. Schiller, K. A. Friedrich, *J. Power Sources* **2018**, *380*, 26.

33. C. E. Frey, Q. Fang, D. Sebold, L. Blum, N. H. Menzler, *J. Electrochem. Soc.* **2018**, *165*, F357.

34. Q. Fang, C. E. Frey, N. H. Menzler, L. Blum, *J. Electrochem. Soc.* **2018**, *165*, F38.

35. N. H. Menzler, D. Sebold, S. Zischke, *ECS Trans.* **2019**, *91*, 719.

36. X. Sun, P. V. Hendriksen, M. B. Mogensen, M. Chen, *Fuel Cells* **2019**, *19*, 740.

37. X. Tong, S. Ovtar, K. Brodersen, P. V. Hendriksen, M. Chen, *ACS Appl. Mater. Interfaces* **2019**, *11*, 25996.

38. F. Monaco, M. Hubert, J. Vulliet, J. P. Ouweltjes, D. Montinaro, P. Cloetens, P. Piccardo, F. Lefebvre-Joud, J. Laurencin, *J. Electrochem. Soc.* **2019**, *166*, F1229.

39. Z. Jiao, E. P. Busso, N. Shikazono, *J. Electrochem. Soc.* **2020**, *167*, 024516.

40. R. J. Aaberg, R. Tunold, M. Mogensen, R. W. Berg, R. Ødegård, *J. Electrochem. Soc.* **1998**, *145*, 2244.

41. M. S. Schmidt, K. V. Hansen, K. Norrman, M. Mogensen, *Solid State Ion.* **2009**, *180*, 431.

42. M. Mogensen, K. V. Hansen, in *Handbook of Fuel Cells*, (Eds. W. Vielstich, H. Yokokawa, H. A. Gasteiger), John Wiley & Sons, Chichester, England, **2009**, p. 543.

43. A. Hauch, S. H. Jensen J. B. Bilde-Sørensen, M. Mogensen, *J. Electrochem. Soc.* **2007**, *154*, A619.

44. *Proc. 13th European SOFC & SOE Forum* , A. Hauch, T. L. Skafte, R. Küngas, M. L. Traulsen, S. H. Jensen, (Eds. E. Ivers-Tiffée, A. Weber), Lucerne, Switzerland, **2018**.

45. M. Riedel, M. P. Heddrich, K. A. Friedrich, *Fuel Cells* **2020**, *20*, 592.

46. S. Ovtar, X. Tong, J. J. Bentzen, K. T. S. Thyden, S. B. Simonsen, M. Chen, *Nanoscale* **2019**, *11*, 4394.

47. T. L. Skafte, J. Hjelm, P. Blennow, C. Graves, *J. Power Sources* **2018**, *378*, 685.

48. A. Hauch, M. Marchese, A. Lanzini, C. Graves, *J. Power Sources* **2018**, *377*, 110.

49. J. Schefold, A. Brisse, H. Poepke, *Internat. J. Hydrogen Energy* **2017**, *42*, 13415.

50. H. Uchida, H. Nishino, P. Puengjinda, K. Kakinuma, *J. Electrochem. Soc.* **2020**, *167*, 134516.

51. C. Graves, S. D. Ebbesen, S. H. Jensen, S. B. Simonsen, M. B. Mogensen, *Nat Mater* **2015**, *14*, 239.

52. S. H. Jensen, C. R. Graves, M. B. Mogensen, Patent WO/2020/201485, published October 8th, **2020**.

53. C. Law, S. W. Sofie, *ECS Trans.* **2010**, *28*, 217.

54. D. R. Driscoll, M. D. McIntyre, M. M. Welander, S. W. Sofie, R. A. Walker, *Appl. Catal. A* **2016**, *527*, 36.

55. A. Atkinson, S. Barnett, R. J. Gorte, J. T. S. Irvine, A. J. McEvoy, M. Mogensen, S. C. Singhal, J. Vohs, *Nat. Mater.* **2004**, *3*, 17.

56. C. Graves, L. Martinez, B .R. Sudireddy, *ECS Trans.* **2016**, *72*, 183.

57. T. L. Skafte, B. R. Sudireddy, P. Blennow, C. Graves, *ECS Trans.* **2016**, *72*, 201.

58. H.-Y. Chen, H.-C. Yu, J. S. Cronin, J. R. Wilson, S. A. Barnett, K. Thornton, *J. Power Sources* **2011**, *196*, 1333.

59. Y. Lei, T.-L. Cheng, H. Abernathy, W. Epting, T. Kalapos, G. Hackett, Y. Wen, *J. Power Sources* **2021**, *482*, 228971.

60. A. Nakajo, G. Rinaldi, P. Caliandro, G. Jeanmonod, L. Navratilova, M. Cantoni, J. Van herle, *J. Electrochem. Energy Convers. Storage* **2020**, *17*, 041004.

61. C. W. Bale, E. Bélisle, P. Chartrand, S. A. Decterov, G. Eriksson, A. E. Gheribi, K. Hack, I.-H. Jung, Y.-B. Kang, J. Melançon, A. D. Petersen, C. Robelin, J. Sangster, P. Spencer, M.-A. Van Ende, *Calphad* **2016**, *54*, 35.

62. G. Rinaldi, A. Nakajo, P. Caliandro, L. Navratilova J. Van herle, *ECS Trans.* **2019**, *91*, 641.